Novel Sensors for Portable Oil Analyzers

Robert W. Brown, Yu-Chung N. Cheng, John D. Chunko, and William C. Condit
Department of Physics
Case Western Reserve University
10900 Euclid Ave.
Cleveland, OH 44106-7079
(216) 368-4010

Wayne A. Bush and Margaret A. Zelina
PREDICT
9555 Rockside Rd.
Cleveland, OH 44125
(216) 642-3223

1998

Abstract: We present progress of research and design in the area of liquid sensors for condition-based maintenance where accurate portable devices for monitoring hydraulic and lubricating fluids are desired. Issues addressed include dielectric modeling, capacitive calculations, a novel 'electrogravity' mechanism, and MEMS (microelectromechanical systems) applications. Measurements of capacitance, of frequency response, of oxidation effects, and of breakdown voltages, all as a function of contaminant concentration, have been carried out.

Key Words: Condition monitoring; lubricant contamination; portable instruments; impedance spectroscopy; numerical computation.

Introduction: We have worked intensively over the past few years to produce portable sensors capable of detecting contaminants at increasingly improved resolution [1]. A portable instrument can provide an indication as to the lubrication condition of an oil without the need for any sample preparation such as a separate measurement or use of any chemicals.

Section I - Present Commercial Instrument and Outline of Paper: The latest PREDICT portable instrument, Navigator v1.0, is based on impedance spectroscopy. It measures the magnitude of the impedance of the system represented by the sensor electrode and the oil sample, at different frequencies. Changes in the permittivity and conductivity of an oil can be observed and differentiated. Four distinct frequencies lying in the .1-120 kHz range, have been chosen as a result of extensive empirical research with known oil samples. The frequencies are as follows: Two low frequency readings (100-500 Hz) are used to find changes, on a logarithmic scale, in the conductivity of the oil. The presence of water dominates these frequencies. One intermediate frequency reading (10 kHz) is still sensitive to conductivity, but now in

an approximately linear fashion. One high frequency (120 kHz) reading is taken to measure changes in the permittivity of the oil. The effects of wear debris increase at the higher frequencies.

The instrument reads data for each frequency and stores it in memory. A baseline is established by running a clean sample. A comparison is then made with the data obtained for a (possibly) contaminated sample, and, if changes are greater than an acceptable tolerance, at any frequency, the sample is rejected ('out of limits') and sent to a laboratory for further analysis. The Navigator v1.0 tolerances have been set empirically such that the calls made by the instrument match independent and calibrated tests at the 80% level. The instrument is designed to give an answer within two minutes.

Contaminants such as oxidation, wear particles, water or any contaminant that has a different dielectric constant than the oil being measured will affect a permittivity measurement. Contaminants such as water, soot, very large (175 μm, say) wear particles, along with depletion of the additive packages in some types of oil, can affect the conductivity of the oil. In some cases, the apparent effect can be much larger than the classical electrostatic calculation, due to electrochemical effects (clouds of counterions surrounding the contaminant particle).

In the present paper, we describe certain experiments and modeling that have been carried out in conjunction with the development of Navigator v1.0 and the next generation of such detectors. At any AC frequency, conductive and capacitive effects can be described together via evaluation of the complex dielectric constant. In the second section, we analyze a simple capacitance measurement in terms of the classical Maxwell-Wagner theory for the dielectric constant at low concentrations. In the third section, modeling is carried out for the electric fields of the electrode configurations used in the sensors. Experiments and the modeling for the frequency spectrum of the sensor capacitance are described in the fourth section. Oxidized oil can also be detected by measuring the phase angle associated with an effective sensor impedance of the sensor. Directions using MEMS technology are also indicated in that section. The combination of the important effects of gravitational settling and local electric fields is delineated along with a wear particle discussion in the fifth section. Concluding remarks comprise the last section.

Section II - Modeling Heterogeneous Dielectric Material: A simple analysis of a colloidal mixture of spherical particles interacting with the suspending medium, is the so-called Maxwell-Wagner (MW) model [2, 3, 4, 5]. The analysis assumes that a small fraction q of an 'impurity phase' with conductivity (σ_p) and dielectric constant (ϵ_p) is dispersed in a fluid with conductivity (σ_m) and dielectric constant (ϵ_m). Under the assumption of a constant electric field, the effective dielectric constant is found in the references to be given by

$$\frac{\epsilon^* - \epsilon_m^*}{\epsilon^* + 2\epsilon_m^*} = q\frac{\epsilon_p^* - \epsilon_m^*}{\epsilon_p^* + 2\epsilon_m^*} \tag{1}$$

with

$$\epsilon^* = \epsilon - j\sigma/\omega \tag{2}$$

and angular frequency ω. We can test this formula against experiments involving simple parallel-plate capacitors. The experimental data corresponding to 'Exp. 1' and a theoretical calculation based on the MW model are compared in Table I. The parallel-plate experiments were performed using an HP 16452A liquid test fixture with an accuracy better than the two digits quoted after the decimal point. In the Maxwell-Wagner calculation, the relative dielectric constant of oil is taken to be 2.2, the relative dielectric constant of water to be 81, and the conductivity of water to be 10^{-4} S/m. While the trends are in the right direction in the comparison found in Table I, the quantitative discrepancies suggest additional factors should be taken into account. The data for 'Exp. 2' will be discussed in section IV.

Table I
Capacitance Values of Contaminant Detectors

Frequency	Concentration	Exp. 1 [a]	MW [b]	Exp. 2	Layers
N/A	0	22.69 pf [g]	N/A	40 pf [c,g]	40.2 pf [c,g]
N/A	0	10.59 pf [h]	N/A	18 pf [f,h]	15.0 pf [f,h]
10 Hz	1000 ppm	22.70 pf	22.76 pf	40.4 pf [c]	N/A
10 Hz	5000 ppm	24.05 pf	23.03 pf	2.54 μf [d,e,f]	6.5 μf [d,f]
100 kHz	1000 ppm	22.69 pf	22.75 pf	40.1 pf [c]	52.0 pf [c]
100 kHz	5000 ppm	22.88 pf	23.01 pf	55 pf [e,f,i]	245 pf [f]

[a] displays the experimental results for a parallel-plate capacitor.
[b] displays the results for the Maxwell-Wagner calculation pertaining to the parallel-plate capacitor Experiment 1.
[c] A prototype I sensor was used with substrate dielectric constant of 10.4.
[d] This value was at 20 Hz.
[e] The time-dependence due to water settling must be considered. The present measurement was taken after 1 hour of settling time dependent.
[f] A prototype II sensor was used with substrate dielectric constant of 4.2.
[g] The values correspond to pure oil.
[h] The values correspond to air.
[i] This value was measured at 1 MHz.

Section III - Capacitance of Dielectric Layers and Coplanar Electrodes: The PREDICT sensor described above has a coplanar geometry where electrode tracings are laid out over single planar surfaces. An increased contaminant presence leads specifically to an increase in the capacitance of the electrode array as it is immersed in the oil.

The coplanar array of interleaved conducting strips is supported by a fiberglass substrate. The rectangular coplanar electrode has approximate dimensions of 5 cm by 5 cm and a thin layer of test oil (with a depth of about 5 mm) is sampled by pouring the oil over the electrode. The observed changes of capacitance (ranging from picofarad to microfarad values) upon introduction of 1000-5000 ppm of water are in

adequate agreement with theoretical modeling. The latter is described next, followed by an experimental discussion. The results of the this work have been used in the development leading to the design of Navigator v1.0.

A two-dimensional Green function method, such as that used in parallel arrays of microstrips, can be employed to obtain a capacitance per unit length, and this leads to an accurate estimate of the total capacitance for those systems having gap distances between strips much smaller than the overall array dimensions and where the contaminant effects are not yet considered. Following the equations in [6, 7], the electrostatic potential V is

$$V(\vec{r}) = \int_{\Omega} G(\vec{r}, \vec{r}')\rho(\vec{r}')d^3\vec{r}' \tag{3}$$

where G is the Green function, ρ is the electric charge density, and Ω denotes the conductor surface over which the charge is distributed. The charge distribution on the given coplanar tracing geometry is found by considering Eq. 3 as an inverse problem [8, 9]. The Green function satisfies a Poisson differential equation:

$$\vec{\nabla}(\epsilon\vec{\nabla}G(\vec{r}, \vec{r}')) = -\delta^3(\vec{r} - \vec{r}') \tag{4}$$

It is assumed that there are several layers above and below the copper coplanar traces building up in the y direction, and the traces may be considered to be infinite along the z direction. Within each layer where the dielectric constant is in fact constant, Eq. 4 reduces to Laplace's equation. In terms of a spectral domain (Fourier transformation of the Green function in the x variable), the solutions to Laplace's equation are the well-known exponential functions in y. The lengthy details of the full solution obtained after the boundary conditions between layers are applied are to be published elsewhere.

A simple analytical form for the Green function in the spectral domain of a special case can be found. If we have only two thick layers with dielectric constants ϵ_1 and ϵ_2 above and below the traces (that is, the heights of two layers are considered to be large compared to the dimensions of the traces), the capacitance of the coplanar electrodes is

$$C = \frac{\epsilon_1 + \epsilon_2}{2\epsilon_0} C_0 \tag{5}$$

where C_0 is the capacitance in free space (itself computed with a Green function method). The computer codes written for a general set of layers can be verified against simple results such as Eq. 5.

Consider two cases with no contaminants for 'Exp. 2' in the top two rows of Table I. One corresponds to a thick oil layer on top of a prototype electrode and the other to the case where the electrode is simply exposed to air, both with finite thickness for their substrates taken into account. The theoretical results agree well with the measurements. The capacitive measurements were again carried out with an HP network analyzer. The slightly higher value for the measurement in air is likely due to humidity.

The response curve in Fig. 1 indicates the thresholds or detection limits of the Navigator v1.0 instrument for water contamination.

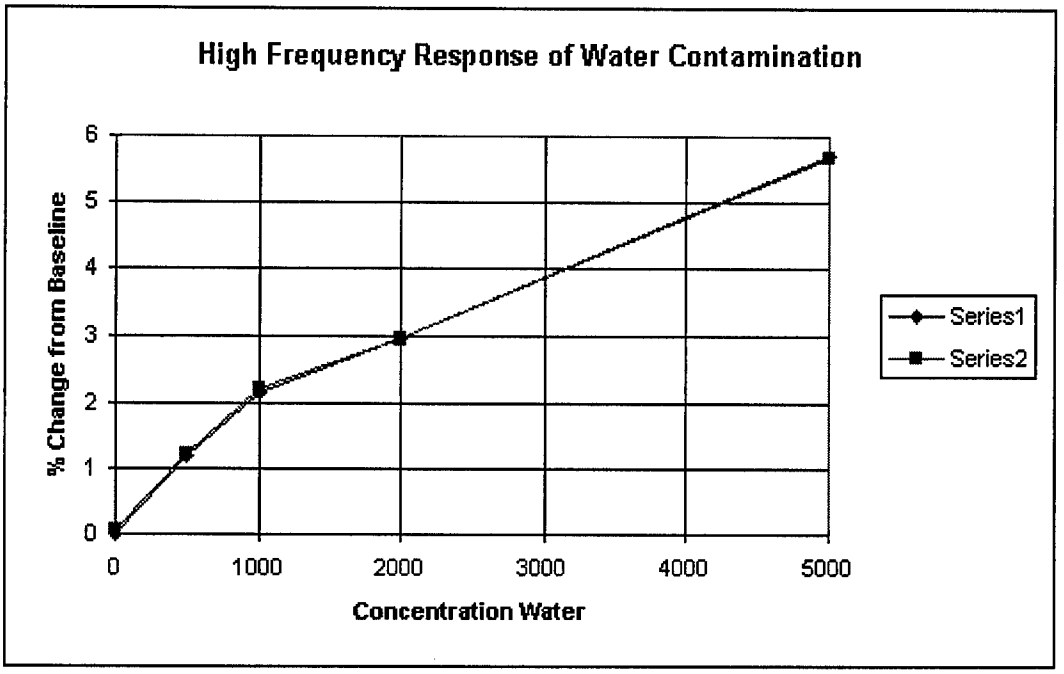

Figure 1: Water response curve of the Navigator v1.0 for 120 kHz. The water concentration is in ppm of oil.

It is observed from the figure that a 0.5% threshold on the high frequency measurement gives an 'out of limits' reading when there has been approximately 250 ppm or more change in the water concentration as compared to a reference oil. The water concentrations in the calibration curve of Fig. 1 are determined with a Water-by-Karl-Fischer titrator (D4928).

Section IV - Frequency Spectrum: We consider now the frequency dependence due to the presence of conductivity in the generalized dielectric constant. At the high frequency end, the conductivity effect is negligible. For lower frequencies, and if there is a nonvanishing conductivity in the layers, then Eq. 2 may be used to generalize the dielectric constants appearing in Eq. 5.

Table II
Capacitances for a water layer

Frequency	C_{exp}	$\|C_{theo}\|$
20 Hz	12.3 ± 0.1 μf	12.3 μf [a]
100 Hz	2.5 ± 0.5 μf	2.46 μf
1 kHz	270 ± 30 nf	246 nf
10 kHz	35 ± 15 nf	24.6 nf
100 kHz	3.4 ± 0.5 nf	2.48 nf
1 MHz	339 ± 19 pf	388 pf

[a] This is fixed by the experimental result.

One example is presented in Table II, where the oil layer is replaced entirely by water. The conductivity in water can be found by fitting the theoretical prediction to the

measurement at 20 Hz, obtaining the value of 3.9×10^{-3} S/m. The capacitances for other frequencies can then be computed. It is seen in Table II that the experimental results and theoretical estimations are in satisfactory agreement.

The next modeling is for two different coplanar traces with 1000 ppm and 5000 ppm water-contaminated oil samples. Columns 'Exp. 2' and 'Layers' in Table I represent the measured and computed results, respectively. The theoretical predictions are based on an assumption that the water has settled into a layer below the oil and on top of the electrodes. Because complete water settling takes a long time, the experimental measurements are smaller than the the computed results. However, there is better than order-of-magnitude agreement and this is impressive when it is recognized that the capacitance changes by six orders of magnitude over a similar change in the frequency range.

It is easy to see the capacitive dependence on frequency ω from an equivalent circuit model for the electrode-sample system, consisting of an effective resistor in parallel with an effective capacitor. When a sample is placed on the sensor, it changes the capacitance C and conductivity. The reactance of the capacitor is $1/(j\omega C)$. Therefore one can see that at a low frequency the reactance is very large and most of the current will flow through the resistor, thus revealing information about the conductivity. When the frequency is higher, the reactance of the capacitor is much less and most of the current will flow through the capacitor, revealing information about the permittivity. Thus one can see how the contributions from conductivity and permittivity can be separated to some degree by changing the frequency.

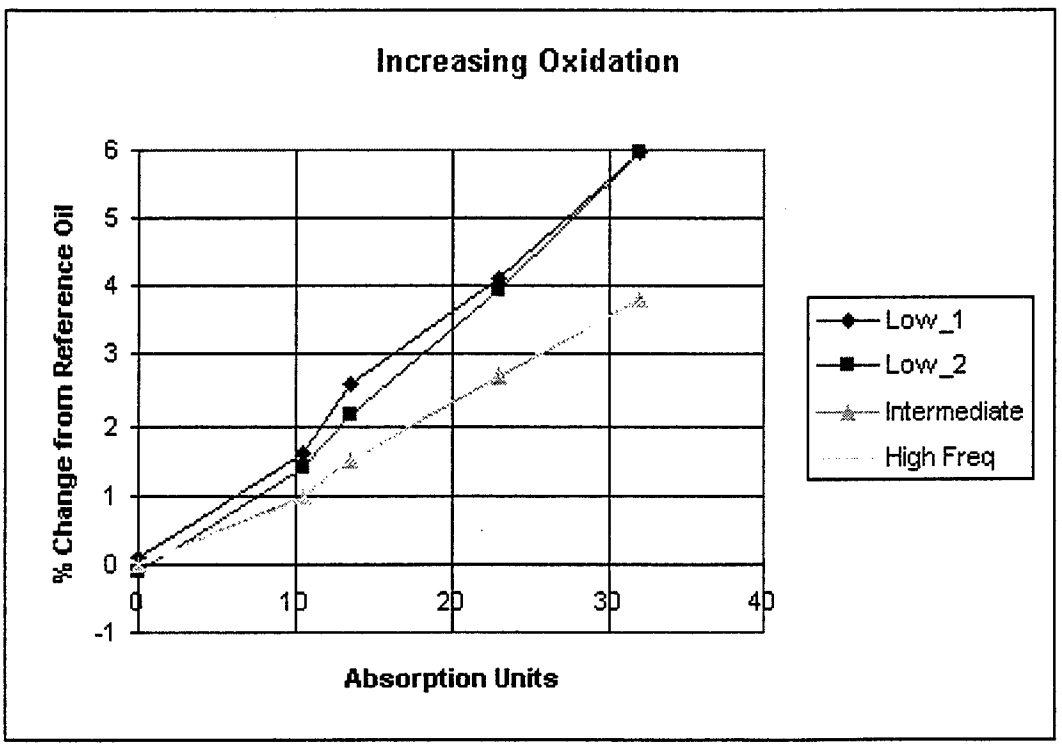

Figure 2: Oxidation Response Curves for Navigator v1.0

Oxidation of oil is an additional industrial problem. The current Navigator v1.0 can be used to detect oxidation levels as well. The response curves in Fig. 2 indicate the thresholds or detection limits of the Navigator v1.0 instrument for oxidation. The tolerance of frequencies are set such that the unit triggers an 'out of limits' reading for a change in 10 AU (absorption units) or more in oxidation. Oxidation is defined in the 1710 cm^{-1} region using a Fourier transform infrared (FTIR) spectrometer which indicates the presence of carboxylic acids in the lubricant.

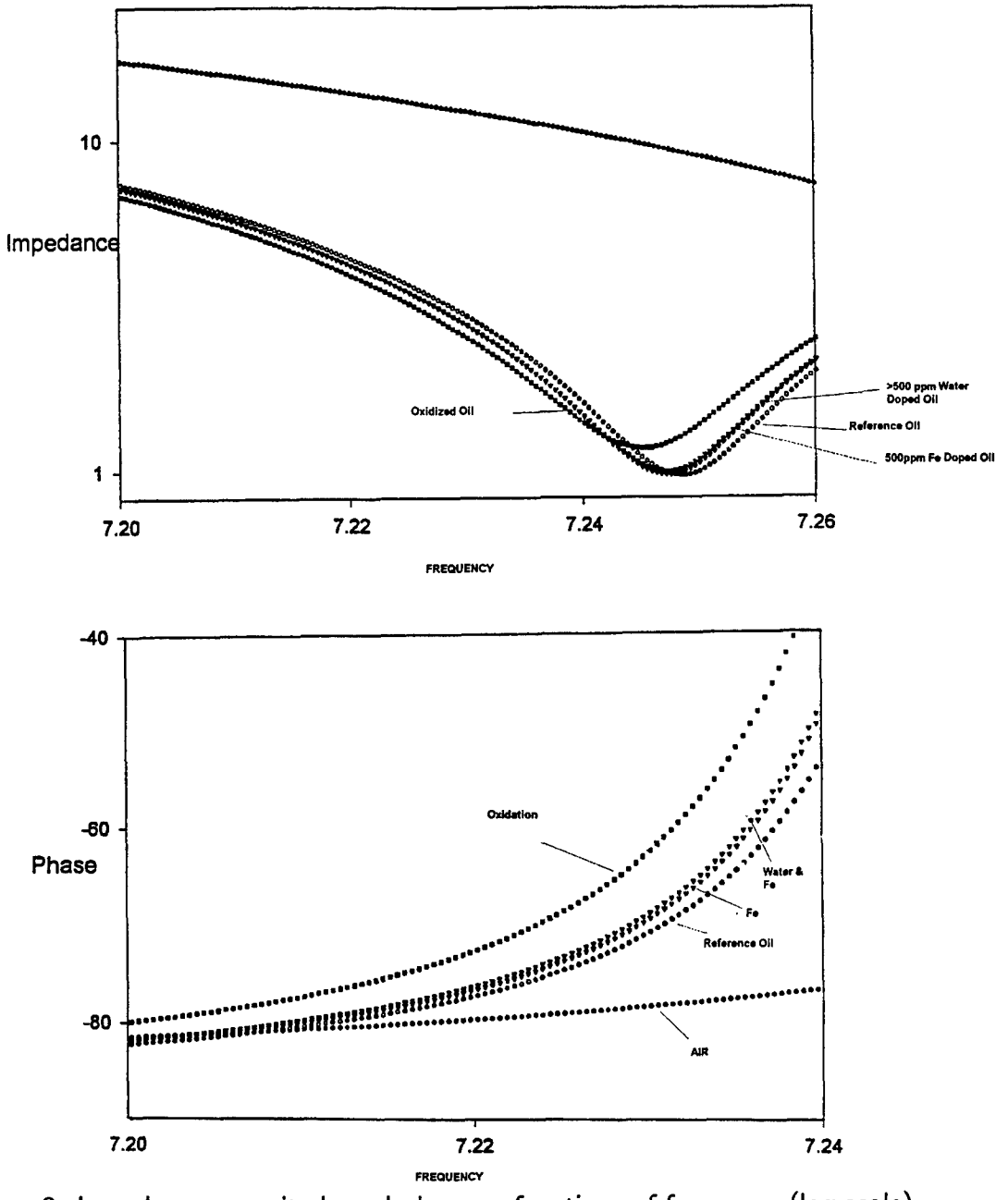

Figure 3: Impedance magnitude and phase as functions of frequency (log scale).

Other methods exist for measuring oxidation. Initial testing indicates that by measuring the phase angle and/or magnitude of the impedance near the resonance of the

grid, oxidation levels can be detected. Changes in an oil molecule caused by increased oxidation suppress the response of the orientation polarization of the molecule to a rapidly changing electric field. At lower frequencies this is not a problem, but at higher frequencies it adds to the loss and thus a reduction in Q and a change in phase. See the phase curves in Fig. 3 near the resonant frequency of the current sensor (20 MHz for an unloaded sensor).

In general, contaminants in the oil change the Q factor of the sensor. For example, doping an oil sample with ferrous wear particles lowers the resonant frequency, but does not appear to affect the bandwidth of the signal. However, oxidized oil both shifts the resonant frequency and increases the bandwidth. Again see Fig. 3 for the impedance magnitude curves.

There is an increasing interest in miniaturization of contaminant sensors for in situ monitoring. The sensor used for impedance spectroscopy with the present commercial instrument has been prototyped using MEMS fabrication techniques at the Case Western Reserve University MEMS laboratory through Ohio MEMSNet. The early prototypes have reduced the large (25 cm^2) scale sensor in the commercial Navigator v1.0 product to 1 mm^2. The impedance spectroscopy sensor fabricated on silicon is termed the MOS device for Miniature Oil Sensor and its applications are patent pending. The prototype devices have been wirebonded and packaged in a variety of housing for tests in real time and in situ applications. Dies have been fabricated specifically for water and oxidation, and a series of dies fabricated specifically for ferrous particle detection.

Section V - Electrogravity and Critical Voltages: Let us turn our attention to wear particle detection. The response curves in Fig. 4 indicate the thresholds or detection limits of the Navigator v1.0 instrument for 60 μm iron-particle concentrations. The thresholds on the corresponding frequencies are set such that the instrument reports an 'out of limits' reading when there is a 400 ppm or more change in Fe from the reference. A single 175 μm particle or a build up of particles amounting to 175 μm across the traces will also trigger 'out of limits.'

More sensitivity in the detection of ferrous particles is desired. To improve matters, we have discovered a technique separate from the capacitive methodology. If we immerse tracer electrodes, such as those used in capacitive sensing, in a wear-particle contaminated oil sample, we will observe current surges (from μA to mA in a typical case) through the electrodes as critical voltages are applied. What happens is that 60 micron particles, say, settle fairly quickly under the combined effects of gravity and the local electrode electric field. The particles tend to form bridges between electrodes, a phenomenon we refer to as 'electrogravity.' Some preliminary experiments have been carried out at this stage. The correlation with particle contamination down to the levels of 100 ppm is very encouraging. The breakdown voltages are in the range of 100-500 V.

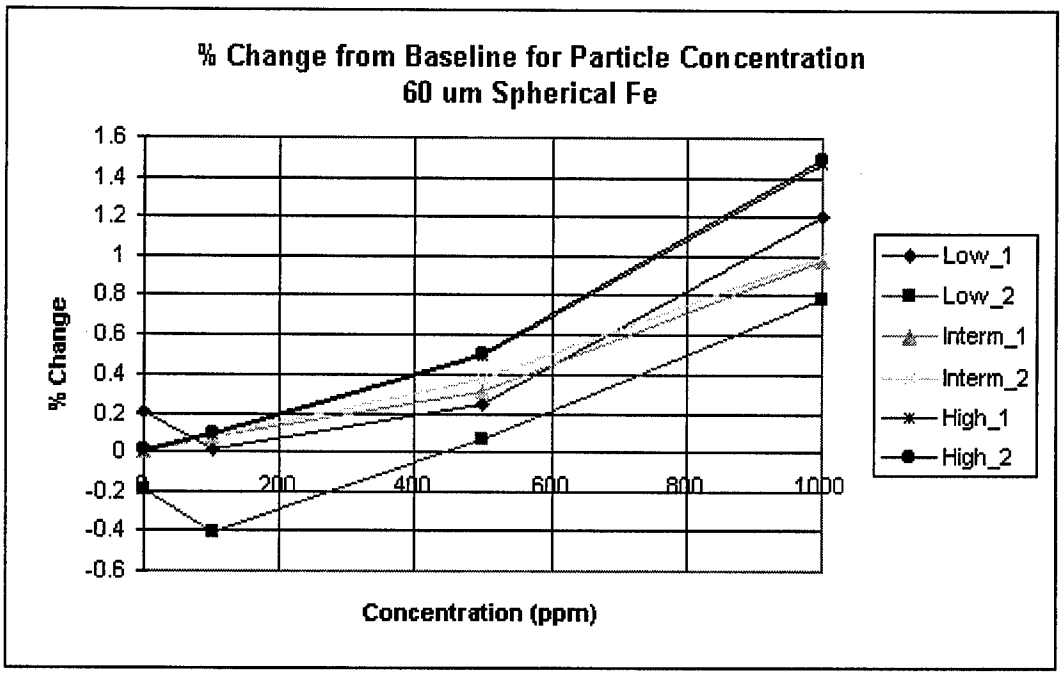

Figure 4: Ferrous Particle Response in Navigator v1.0

Section VI - Conclusions and Outlook: In predictive maintenance, changes in contaminant levels on the order of 100 ppm are of increasing significance. Toward this end, we have achieved a magnitude of order increase in the gain of the sensor from that of other sensors on the market by maximizing the capacitance per unit area of the sensor.

Reading the oil at four frequencies enables the instrument to separate changes in the conductivity and permittivity caused by contaminants. Also different types of oil have different characteristic spectrum, and with a little experience a user can differentiate between them. This is an obvious area for periodic software enhancements.

While the MW theory showed capacitive changes in the right direction for the contaminant modeling, we have found interesting deviations from this behavior. Equation 1 does not take into account synergistic effects between the contaminant and the base dielectric (oil), such as 'conduction hopping' of current carriers from one conducting contaminant particle to another, or, at higher electric fields, the lowering of the breakdown strength by contaminant particles. It does not account for the effect of contaminants which go into a true solution in the base oil (such as anti-oxidants). It may be useful to study these rather sensitive physical/chemical properties for a wide variety of lubricating oils, and establish proper operating regimes for 'combined sensors' which utilize information from dielectric constant, dielectric strength, and conductivity measurements. Additionally, it is useful to study purely mechanical effects (the settling of suspensions) to augment the electrical measurements and provide additional information.

Even at low operating voltages, apparent electrophoretic separation of the oil and

water is occasionally seen when a sample is left under applied fields for times of more than a few minutes. Thus we have already seen signs of gross electrical flow effects on fluid contaminants which we expect to become much stronger at higher electric fields. A suggestion in this paper is the intentional use of these electrophoretic or dielectrophoretic effects, rather than the disregarding of them as a nuisance.

Future MEMS work includes a next prototype run on SiC allowing for higher operating temperatures. The need for very high in situ operating temperatures for some systems is driving us to investigate MEMS photolithography with refractory metals. Incorporation of the voltage breakdown work is planned for applications in silicon. Packaging of this sensor in an existing engine plug is also being investigated.

Goals in the breakdown work are to reduce the high critical voltages required, and to reduce the waiting time under the gravity effect. The modeling of the phenomenon involves the calculation of the electric field and the application of Poisson statistics to find the optimum depth of oil layers in the sensor container. Our experimental results agree with preliminary estimates from Poisson statistical analysis. The present aim is to detect 100 ppm of 10-micron particles in oil. A principal emphasis for the future is the advancement of wear-particle sensors.

References:

[1] R. W. Brown and Y.-C. N. Cheng, "Mathematical-physics optimization of electrical sensors for contaminant detection," presented at 7th Annual User's Conference, Las Vegas, NV, October 20-23, 1996. This is an earlier progress report of the CWRU-PREDICT research activity.

[2] V. V. Daniel, *Dielectric Relaxation.* New York: Academic Press, 1967.

[3] B. K. P. Scaife, *Principles of Dielectrics.* Oxford: Clarendon Press, chap 4, 1989.

[4] E. Haslund, B. D. Hansen, R. Hilfer, and B. Nost, "Measurement of local porosities and dielectric dispersion for a water-saturated porous medium," *J. Appl. Phys.*, vol. 76 No. 9 pp. 5473-5480, 1994.

[5] G. Blum, H. Maier, F. Sauer, and H.P. Schwan, "Dielectric relaxation of colloidal particle suspensions at radio frequencies caused by surface conductance," *J. Phys. Chem.*, vol. 99 No. 2, pp. 780-789, 1995.

[6] W. Delbare, and D. De Zutter, "Space-domain Green's function approach to the capacitance calculation of multiconductor lines in multilayered dielectrics with improved surface charge modeling," *IEEE Trans. Microwave Theory and Tech.*, vol. 37 No. 10, pp. 1562-1568, 1989.

[7] K. S. Oh, D. Kuznetsov, and J. E. Schutt-Aine, "Capacitance computations in a multilayered dielectric medium using closed-form spatial Green's functions," *IEEE Trans. Microwave Theory and Tech.*, vol. 42 No. 8, pp. 1443-1453, 1994.

[8] M. N. O. Sadiku, *Numerical techniques in electromagnetics.* Boca Raton, Fla.: CRC Press, 1992.

[9] W. H. Press, B. P. Flannery, S. A. Teukolsky, and W. T. Vetterling, *Numerical Recipes in FORTRAN: the art of scientific computing.* Cambridge [England]: Cambridge University Press, 1994.